Agricultural Water Management 273 (2022) 107918

Contents lists available at ScienceDirect

Agricultural Water Management

journal homepage: www.elsevier.com/locate/agwat

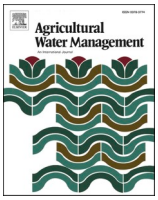

Evolution, severity, and spatial extent of compound drought and heat events in north China based on copula model

Qi Zhang [a,*], Xin Yu [a], Rangjian Qiu [b,*], Zhongxian Liu [a], Zaiqiang Yang [a]

[a] Jiangsu Key Laboratory of Agricultural Meteorology, School of Applied Meteorology, Nanjing University of Information Science and Technology, Nanjing 210044, China
[b] State Key Laboratory of Water Resources and Hydropower Engineering Science, Wuhan University, Wuhan, China

ARTICLE INFO

Handling Editor - Dr. B.E. Clothier

Keywords:
Compound events
Copula model
Standardized precipitation index
Standardized temperature index
North China

ABSTRACT

Compound drought and heat (CDHE) is frequently occurred worldwide and leads to disproportionate impacts on agricultural production than univariate climate extremes, hence continues to receive research attention. However, the driving mechanism and occurrence characteristics of CDHEs remain unclear in some agro-ecological sensitive regions. Here, we adopted standardized precipitation index (SPI) and standardized temperature index (STI) to identify the intensity of drought and heat, respectively, in north China, and then to identify the month and area that most prone to CDHEs. Copulas can simulate the dependence between variables, hence were proposed to construct joint cumulative probability distributions of SPI and STI, so as to simulate the occurrence characteristic of CDHEs. The results demonstrated that in cold season, there were some stations with significant positive correlations between the SPI and STI. However, ~ 80 % of stations had significant negative correlations between the two variables in July (the month of the year with the most stations). Hence, July is considered as the month most prone to CDHEs among the year in north China. We also found that the Symmetrized Joe-Clayton copula was the best to construct joint probability distributions of SPI and STI in most stations. In July, CDHEs occurred more frequently after 1990s with much higher intensity and wider spatial extent, which was mainly attributed to more severe heats. Spatially, mid-western plain and north mountainous areas were more prone to CDHEs. Our findings provide a better understanding of CDHEs in north China and could offer valuable references for meteorological disaster risk prevention in agriculture production.

1. Introduction

Climate extremes continues to receive research attention due to their disproportionate impacts on society and agroecosystem (IPCC, 2012). Especially, some of the most serious impacts are often caused by a combination of climatic extremes that termed as 'compound event' (IPCC, 2013). Compound events involve more than one variable (Zscheischler and Seneviratne, 2017), which usually have excessive impacts than univariate climate extremes. Drought and extreme heat often co-occurred under global warming, which is one of the most concerned compound events types. Compound drought and heat event (CDHE) seriously affected vegetation production (Ciais et al., 2005; De Boeck et al., 2011; Wolf et al., 2016), caused tree mortality (Allen et al., 2010), promoted insect outbreaks (Williams et al., 2010), and wildfires (Flannigan et al., 2009), negatively affected agriculture sector. In addition, extreme heat and dry conditions are conducive to the spread of diseases, and thus severely affect human health (Chretien et al., 2007; Padmanabha et al., 2010; Bandyopadhyay et al., 2012). Therefore, understanding concurrent characteristics of compound drought and heat events is of crucial importance to provide relevant information for disaster mitigation.

Former studies mainly focus on investigating the disasters from univariate perspective, hence leading to underestimate the impacts of compound events. The magnitudes of individual hazards will increase as climate extremes co-occurred (Shukla et al., 2015; AghaKouchak et al., 2014; Griffin and Anchukaitis, 2014). In addition, drought and extreme heat interact with each other. For instance, surface drought caused by precipitation deficit can induce less evaporation, leading to atmospheric heating. Mueller and Seneviratne (2012) found that the number of high temperature days is closely related to the previous lack of precipitation in many parts of the world. On the other hand, extreme heat will significantly increase evaporation demand, thereby exacerbating the severity of drought (Dai, 2013). This can also explain why CDHE is one of the most frequent types of compound events under global warming.

* Corresponding authors.
E-mail addresses: zhangq861206@126.com (Q. Zhang), qiurangjian@whu.edu.cn (R. Qiu).

https://doi.org/10.1016/j.agwat.2022.107918
Received 16 June 2022; Received in revised form 27 August 2022; Accepted 30 August 2022
Available online 5 September 2022

In recent years, there were some studies concerning compound events (Ridder et al., 2020; Zscheischler et al., 2020). The most common approach was to define and identify the compound events, so as to analyze the spatial and temporal distributions of historical occurrence frequencies (Chen and Li, 2017; Wu et al., 2019b; Zhang et al., 2020). In different studies, the definitions may be different. For instance, Zhang et al. (2020) defined the short-term concurrent drought and heatwave events from evapotranspiration, soil moisture and surface temperature to study their historical occurrence frequency around the world. Wu et al. (2019b) used 25th percentile of precipitation and 75th percentile of temperature to define compound precipitation and temperature extreme events in China. This is a straight forward approach to improve our understanding of compound events in history. However, as the compound events are extreme events, this kind of studies always require long-term series data to contain more samples. Moreover, because compound events are multi-variable issues, this kind of studies didn't capture the dependence structure between variables, which is essential in estimating the probability of compound events and their potential effects (Hao et al., 2018).

Some other studies on compound events used multivariate joint distribution to simulate the dependence between variables, and to present the occurrence probability of compound events. Among them, the copula models are the most commonly used, especially for bivariate issues (Zscheischler and Seneviratne, 2017; Chen et al., 2019; Ribeiro et al., 2020; Collins, 2021). In high dimensions, meta-Gaussian model has been proposed (Hao et al., 2018). Before performing joint distribution for two or more variables, the marginal distribution of univariate must be fitted separately. The advantage of copulas is allowing the correlate variables without the necessity of similar marginal distributions (Wazneh et al., 2020). In the studies of CDHEs, the marginal distributions of precipitation (Collins, 2021) or some drought indexes, such as standardized precipitation index (SPI) (Hao et al., 2018), Palmer drought severity index (PDSI) (Chen et al., 2019), were fitted to denote drought (water deficit), and the marginal distributions of maximum temperature (Collins, 2021), the number of high temperature days (Chen et al., 2019; Ribeiro et al., 2020) were commonly used to denote extreme heat. However, the indexes to denote drought and heat in the joint probability modeling were not comparable. For example, drought indexes are commonly standardized but heat indexes are not. This may have potential adverse effects on exploring the dominant drivers of compound events and the dependence between variables. So far, the exploration of concurrent event is increasing. However, the existing studies were most on global or national scale, targeted researches on some sensitive and vulnerable agricultural areas are still missing. In addition, the driving mechanism and occurrence characteristics of CDHEs in these areas are remain unclear. Moreover, the current methodology applied to investigate compound events has some defects as described above.

Hence, in this study, CDHEs were studied in north China, which is susceptible to CDHEs and is a major agriculture area in China (Kang and Eltahir, 2018). Two comparable indexes, SPI and standardized temperature index (STI), were adopted to denote intensities of drought and heat, respectively. Copulas were used to link the marginal distributions of the two variables, which can capture the dependence between variables. The main objectives were (1) to identify the most frequently occurred month and areas of CDHEs across north China during period 1961–2019; (2) to explore the dominant driven factor of interannual variation of CDHEs; and (3) to study the spatial distributions of joint return periods of CDHEs with different drought and heat intensities.

2. Dataset and methodology

2.1. Study area

The north China (112.1–122.42°E, 34.22–42.35°N) consists of Beijing, Tianjin, Hebei, Shandong, and northern Henan, with an area of ~ 400, 000 km^2 (Fig. 1). It is the most important winter wheat and summer maize production area in China. This region has a temperate continental monsoon climate, which is cold and dry in winter, and hot and rainy in summer. Seventy percent of the annual precipitation occurs from June to September with large interannual variability, hence there is frequently drought. Because north China plain has experienced great expansion of irrigated agriculture with significant impact on the surface temperature, the risk of high temperature and heatwave in north China has increased since 1970 (Kang and Eltahir, 2018). Owing to climate change and human interference, this region is more prone to CDHEs, and the potential losses for agricultural production are huge.

2.2. Dataset

The dataset including daily precipitation and average temperature data from 39 national weather stations during the period 1960–2019 was collected from China Meteorological Data Network (https://data.cma.cn/site/index.html), which has been performed rigorous quality control procedures. It is one of the best daily meteorological datasets in China (Chen and Li, 2017), and is widely used (Qiu et al., 2021b, 2022).

2.3. Methods

2.3.1. Definition of compound drought and heat events

In this study, we investigated the monthly CDHEs. For a certain month, when drought and heat happened simultaneously, this month can be defined as CDHE occurred. Four characteristics of CDHEs in different time periods are evaluated in this study: intensity, dominated factor, spatial extent, and joint return period. We studied the intensities of drought and heat in the CDHEs, if heat intensity is higher than its drought intensity, this CDHE can be defined as heat dominated. The spatial extent of CDHEs in a certain month is defined as the proportion of stations with compound events happened in north China in that month. Risk of CDHEs is expressed by its return period. A region with shorter return period means this region is more prone to CDHEs and with higher risk.

To identify the drought, a commonly used index, SPI, was selected. The main advantage of using SPI is that it can be compared across different locations and calculated at various timescales. To calculate SPI, the data of precipitation are fitted by the gamma distribution, then converted to the standard normal distribution. Droughts are the

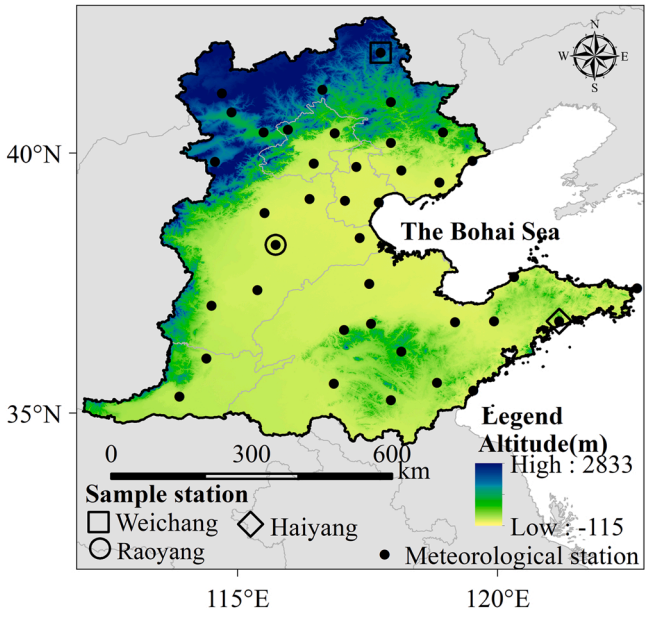

Fig. 1. Location of north China and distribution of meteorological stations.

negative anomalies when SPI < -0.5 (McKee et al., 1993). Detailed calculation processes can be found elsewhere (Yao et al., 2018). Since heat is closely related to the previous lack of precipitation (Mueller and Seneviratne, 2012), SPI were calculated at 1-, 2-, 3-, 4-, 5-, 6-, 9-, 12-month timescales in this study, so as to investigate the timescale of drought most closely related to heat. To identify heat, we adopted the STI index, which is computed in a similar spirit with SPI (Zscheischler et al., 2014). Since temperature anomalies can be assumed to be normally distributed (Hansen et al., 2012; Zscheischler et al., 2014), time series of monthly average temperature can be directly fitted by a normal distribution to calculate STI. Heat is defined as the positive anomalies when STI > 0.5. According to previous studies (McKee et al., 1993; Zscheischler et al., 2014), categories of drought/heat intensity based on SPI/STI can be divided into four levels, as shown in Table 1. Hence, 16 corresponding bivariate permutations are generated. We will examine CDHEs of these 16 drought and heat intensity combinations. In this study, the opposite values of SPI (-SPI) were used to represent the drought intensity, hence, higher value of -SPI represents stronger drought. This makes it more convenient for subsequent fitting of probability distributions.

2.3.2. Copulas and bivariate joint return periods

Any multivariate joint distribution can be written in terms of univariate marginal distribution functions and a joint model, such as copula, which describes the dependence structure between variables (Nelsen, 2007). Copula enables the flexible selection of arbitrary marginal distribution structures (Xu et al., 2021) and has been widely used in hydrology and meteorology (Mellak and Souag-Gamane, 2020; Zhang et al., 2021a; Zhu et al., 2019). One of the objectives of this study is to estimate the joint cumulative probability distribution of CDHEs. Six copula functions are evaluated to link the marginal distributions of drought (denoted by -SPI) and heat intensities (denoted by STI). The specific functions and parameter ranges are shown in Table 2. The Akaike Information Criterion (AIC) is used to illustrate the fitting goodness of the six copulas (Akaike, 2011). In this study, the candidate univariate marginal distributions include the normal distribution (NORM), the extreme value distribution (EV), and the generalized extreme value distribution (GEV). The Kolmogorov-Smirnov test (K-S test) is used to select the optimal marginal distribution function (Massey, 1951), and p-value near to 1 indicates the marginal distribution function fits the data very well. The K-S test is also used to assess the differences between the cumulative distribution functions (CDFs) of compound events in different time periods. p-value < 0.05 indicates the data from the two periods are draw from different distributions at a 0.05 significance level.

The bivariate joint return periods of CDHEs are computed from the fitted copulas. The two-dimensional exceeding probability is the probability of an event that both variables exceed given thresholds, which can be denoted as follows (Zscheischler and Seneviratne, 2017):

$$p = \mathrm{P}(X > x \cap Y > y) = 1 - u - v + C(u, v) \tag{1}$$

where X and Y are the random variables, i.e. -SPI and STI in this study; x and y are the given thresholds; u and v are the cumulative probabilities when the random variables X and Y are less than the thresholds x and y, calculated by the best fitted marginal distribution functions. The joint return periods (RP) related to the exceeding probability p can be computed as:

$$\mathrm{RP} = 1/p \tag{2}$$

Table 1
The categories of drought/heat intensity denoted by SPI/ STI.

Drought/Heat category	SPI ranges	STI ranges
Mild	$-1.0 \leq \mathrm{SPI} < -0.5$	$0.5 \leq \mathrm{STI} < 1.0$
Moderate	$-1.5 \leq \mathrm{SPI} < -1.0$	$1.0 \leq \mathrm{STI} < 1.5$
Severe	$-2.0 \leq \mathrm{SPI} < -1.5$	$1.5 \leq \mathrm{STI} < 2.0$
Extreme	$\mathrm{SPI} < -2.0$	$\mathrm{STI} > 2.0$

3. Results

3.1. Determination of the month most prone to CDHEs

For each station and each month, SPI were calculated at 1-, 2-, 3-, 4-, 5-, 6-, 9-, 12-month timescales. Correlation analysis was conducted between 1-month scale STI (STI_1) and SPIs on each timescale, so as to investigate the timescale of drought most closely related to heat and the months in which CDHEs were most likely to occur. Proportions of stations with significant correlations ($p < 0.05$) between STI_1 and SPIs were displayed in Fig. 2. Significantly positive correlations mainly appeared in cold season, and the largest proportion of stations with significantly positive correlation was 28 %, which occurred between STI_1 and SPI_4 (SPI on 4-month scale) in December. This means that after a period of precipitation deficit (lower SPIs), it more likely accompanied by lower temperatures (lower STIs) in cold months. From March to September, the significant correlations between STI_1 and SPIs on different timescales were all negative. In June and July, the ratios of stations having significantly negative correlations were obviously greater than that in other months, and that in July (generally > 0.8) were obviously greater than in June. This indicates that heats (higher STIs) in June and July are likely to be accompanied after a period of precipitation deficit (lower SPIs) in north China, leading to high risk of CDHEs. The largest ratio of stations with significantly negative correlation appeared between STI_1 and SPI_3 in July. Hence, July can be determined as the month most prone to CDHEs, and 3-month scale drought is most closely related to heat in July. In the following sections, we will take SPI_3 in July as an example to study the characteristics of CDHEs.

3.2. Construction of bivariate joint distribution of -SPI and STI by using copulas

In north China, stations with significantly negative correlations between STI_1 and SPI_3 in July are denoted by colored circles in Fig. 3, which are prone to CDHEs. Stations denoted by grey circles are not studied as they don't have significant correlation between STI and SPI. As shown in Fig. 3, GEV is the optimal marginal distribution function for both SPI and STI at most stations, and NORM performs the best at some other stations. The p-value of K-S test for marginal distribution of STI at each station is between 0.58 and 0.99 (Fig. 3a), and is between 0.29 and 0.99 for SPI (Fig. 3b), indicating a better performance of the marginal distribution for STI than for SPI. Six different copulas are used to link the marginal distributions of STI and -SPI at each station, and AIC is used to select the best copula function. Fig. 4 shows that the Symmetrised Joe-Clayton copula is the optimal copula at most stations, followed by Student's t, Frank, and Gumbel copula.

Three sites, which represented different geographical background, are selected as examples to show the joint cumulative probability distributions of STI and -SPI fitted by the optimal copula function (Fig. 5). The three sites are Weichang, Haiyang, and Raoyang, located in northern mountainous area, east costal area, and mid-western plain area, respectively. From the optimal copula functions, we can obtain the joint cumulative probability at any STI and -SPI. CDHE is the part that both values of -SPI and STI over 0.5. For example, the probability of drought and heat intensity simultaneously < 0.5 is 0.58 at Weichang and 0.51 at Haiyang. Fig. 5 also reveals that the increasing trend of cumulative probability with increasing drought intensity is similar at the three stations. However, this is not the case for heat intensity. For Weichang and Raoyang, the cumulative probability remains near zero when heat intensity is < -2, and the probability slightly increase when heat intensity is > 2. However, for the Haiyang, cumulative probability stops to further increase when heat intensity is > 2. This indicates extreme heat

Table 2
Summary of bivariate copula functions.

Copula	$C(\mu, \nu)$	Parameter range
Frank	$-\frac{1}{\theta}\ln\left[1+\frac{(e^{-\theta\mu}-1)(e^{-\theta\nu}-1)}{e^{-\theta}-1}\right]$	$\theta \neq 0$
Clayton	$(\mu^{-\theta}+\nu^{-\theta}-1)^{-\frac{1}{\theta}}$	$\theta \in [0,\infty]$
Gumbel	$\exp\left\{-[-\ln\mu)^{\theta}+(-\ln\nu)^{\theta}]\right\}$	$\theta \in [1,\infty]$
Student's t	$t_{\kappa+1}\left(\frac{t_{\kappa}^{-1}(\mu)-\theta t_{\kappa}^{-1}(\nu)}{\sqrt{\frac{\left(\kappa+\left(t_{\kappa}^{-1}(\nu)\right)^2\right)(1-\theta^2)}{\kappa+1}}}\right)$	$\kappa > 0 \quad \theta \in [-1,1]$
Plackett	$\frac{1}{2(\theta-1)}\left\{1+(\theta-1)(\mu+\nu)-[1+(\theta-1)(\mu+\nu))^2-4\theta(\theta-1)\mu\nu\right]^{\frac{1}{2}}\}$	$\theta \geqslant 0$
Symmetrised Joe-Clayton	$1-\left((1-\mu)^{\theta}+(1-\nu)^{\theta}-(1-\mu)^{\theta}(1-\nu)^{\theta}\right)^{-\frac{1}{\theta}}$	$\theta \geqslant 1$

Note: C (μ, ν) is the joint cumulative probabilities by copulas; μ and ν are the marginal distributions of -SPI and STI, respectively; θ is the copula parameter.

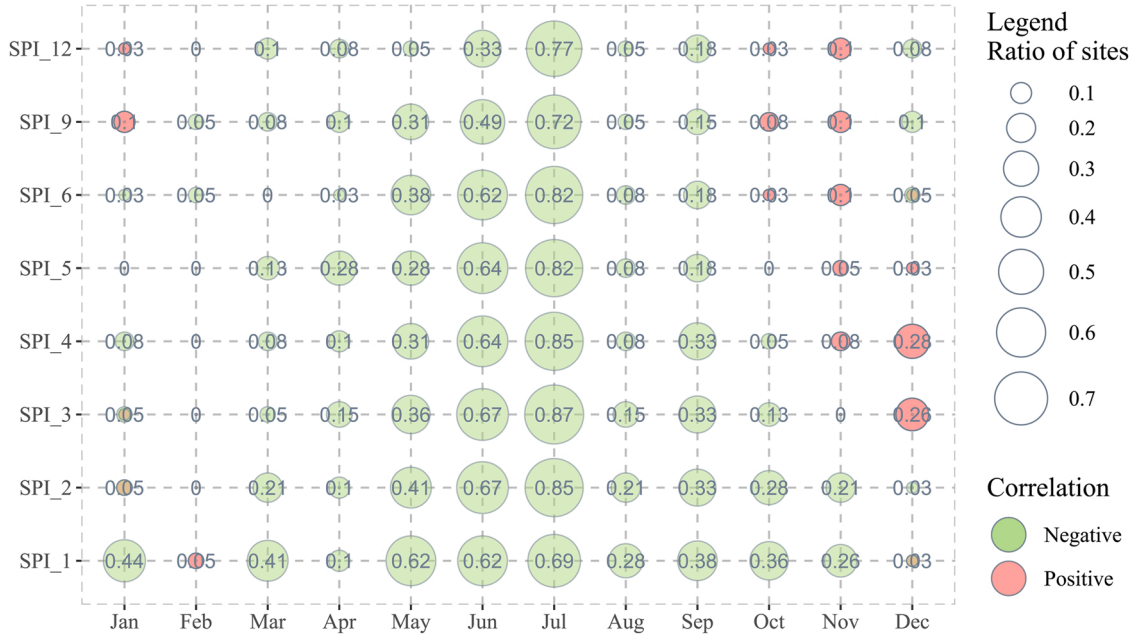

Fig. 2. Ratio of stations with significant correlations ($p < 0.05$) between STI_1 and SPIs on different timescales in each month. Size of the bubbles denote the ratios of stations with significant correlations. Green bubbles denote negative correlation and pink bubbles denote positive correlation. If bubbles of the two colors overlap, it denotes some sites are positively correlated and some sites are negatively correlated.

events rarely occurred in Haiyang.

Based on Eq. (2) and the best fitted copula function, joint return period of CDHEs at any drought and heat intensity can be calculated. We also take Weichang, Haiyang, and Raoyang as examples to show the isolines of the five selected joint return periods. Fig. 6 shows that compared to the other two stations, the isolines at Haiyang are more densely distributed in the direction of heat intensity. This suggests that for CDHEs with the same joint return periods, if their drought intensities are also the same, the compound events in Weichang and Raoyang need more intense heat than in Haiyang. For example, for a CDHE with 50-year return period, its drought intensity is 1.0, the corresponding heat intensity is 1.6 in Haiyang, while 2.3 and 2.2 in Weichang and Raoyang. Fig. 6 also shows that the number of years that CDHEs happened in Weichang, Haiyang, and Raoyang during 1960–2019 are 9, 9, and 11, respectively, and the majority of them happened since 1990.

3.3. Characteristics of compound drought and heat events in different time periods

Characteristics of CDHEs during different time periods are investigated. As shown in Fig. 7a, the frequency of CDHEs in north China obviously increased, the frequency in 2000–2019 was more than twice as that in 1960–1979. In addition, the frequency of CDHEs dominated by heat was obviously increased, however the frequency of CDHEs dominated by drought did not change much. The CDFs of heat intensity (STI) of CDHEs during 2000–2019 and 1980–1999 shifted to right relative to the period 1960–1979 (Fig. 7b). However, the CDF of drought intensity (-SPI) of CDHEs during 2000–2019 slightly shifted to left with respect to the period 1960–1979 (Fig. 7c). This suggests that heat intensities of CDHEs substantially increased, while their drought intensities slightly reduced during 2000–2019 relative to 1960–1979. This explains why more CDHEs dominated by heats in 2000–2019. Fig. 7d shows that the CDF of joint return periods of CDHEs during 2000–2019 slightly shifted

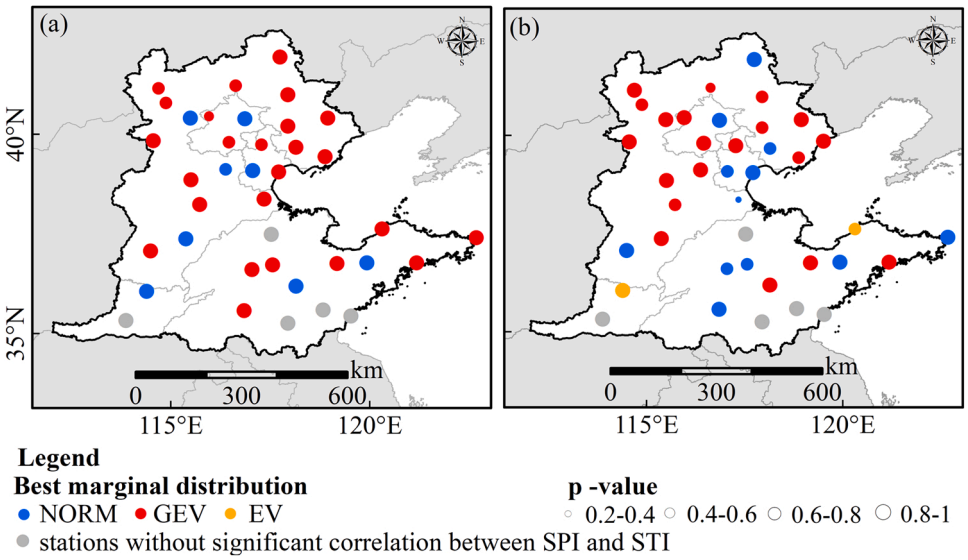

Fig. 3. Optimal marginal distribution function at each station for (a) STI and (b) SPI.

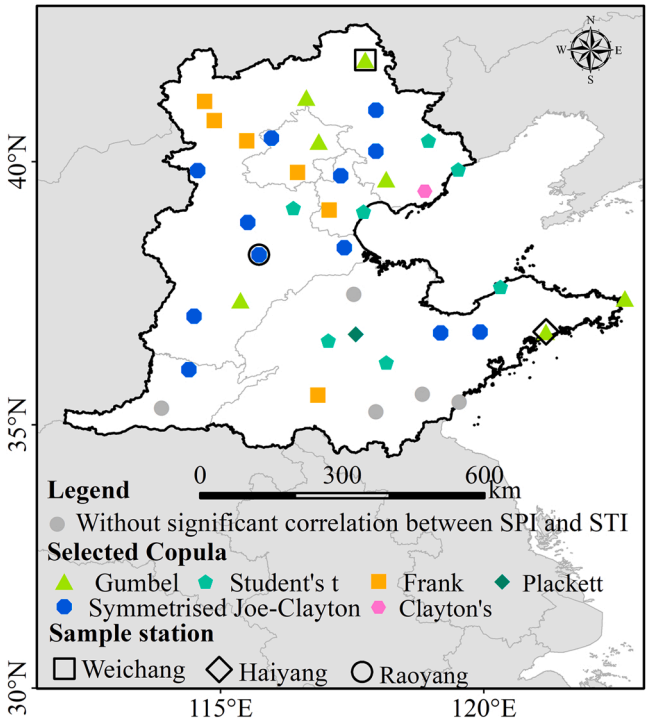

Fig. 4. The selected optimal copula function at each station.

to right relative to the period 1960–1979, indicating more extreme CDHEs in 2000–2019. CDFs in Fig. 7e show that the CDHEs in 2000–2019 had much wider scope than previous periods. All in all, the above results reveal that more frequent CDHEs happened in 2000–2019 with respect to 1960–1979, and the CDHEs with higher intensity and wider spatial extent were appeared in 2000–2019, which were mainly attributed to much serious heats.

3.4. Joint return periods of CDHEs with different drought and heat intensities

The joint return periods of CDHEs for 16 combinations of drought and heat intensity levels in north China are shown in Fig. 8. CDHEs with mild drought and mild heat have the shortest joint return periods, which are generally less than 10 years (Fig. 8a). Joint return periods increased with the increase of either heat intensity or drought intensity. CDHEs with extreme drought and heat seldom happened in north China with the joint return periods over 100 years in most regions (Fig. 8p). Spatially, joint return periods of CDHEs are relatively shorter in mid-western plain area and part of north mountainous area than in other areas, indicating higher risk of CDHEs. What's more, the joint return periods of CDHEs in these two areas are more sensitive to drought intensity than heat. As the increase of drought intensity, the joint return period is much longer than that with the increase of heat intensity. For instance, the joint return periods of CDHEs with extreme drought (Fig. 8m) are longer than that with extreme heat (Fig. 8d) in these two area. In other regions, the joint return periods of CDHEs are relatively more sensitive to heat intensity.

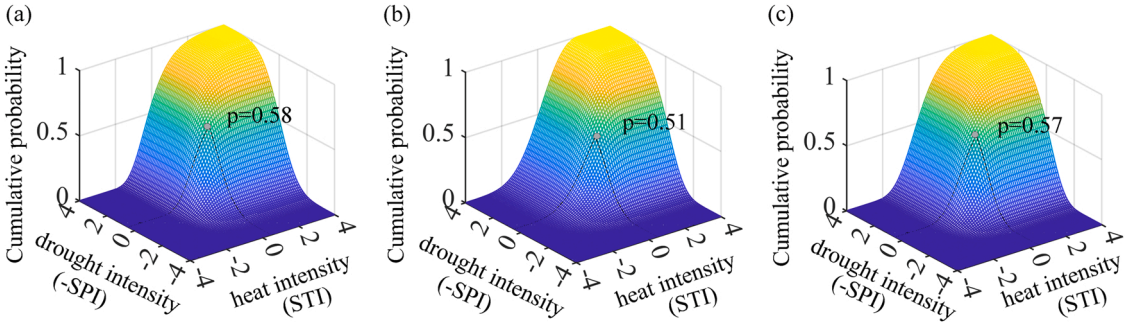

Fig. 5. Joint cumulative probability distributions of drought and heat intensities at (a) Weichang, (b) Haiyang, and (c) Raoyang.

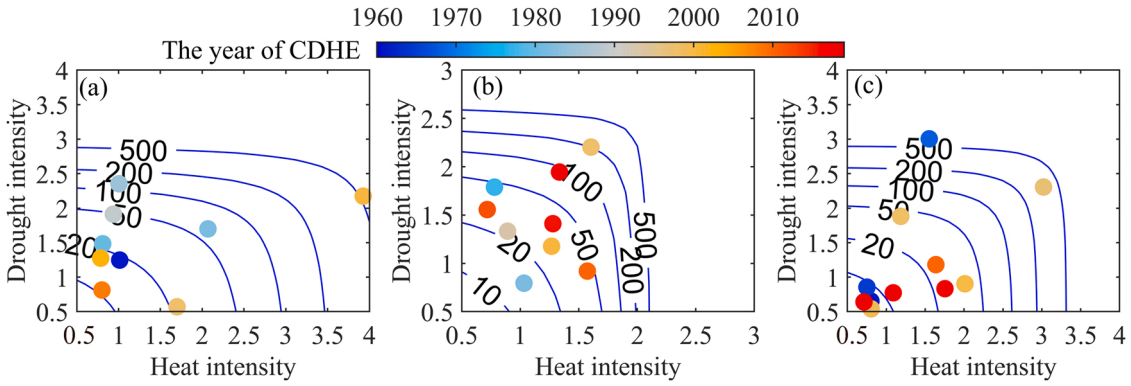

Fig. 6. Isolines of joint return periods (-yr) of compound drought and heat events at (a) Weichang, (b) Haiyang, and (c) Raoyang. Dots in different colors indicate the years in which CDHEs occurred during 1960–2019.

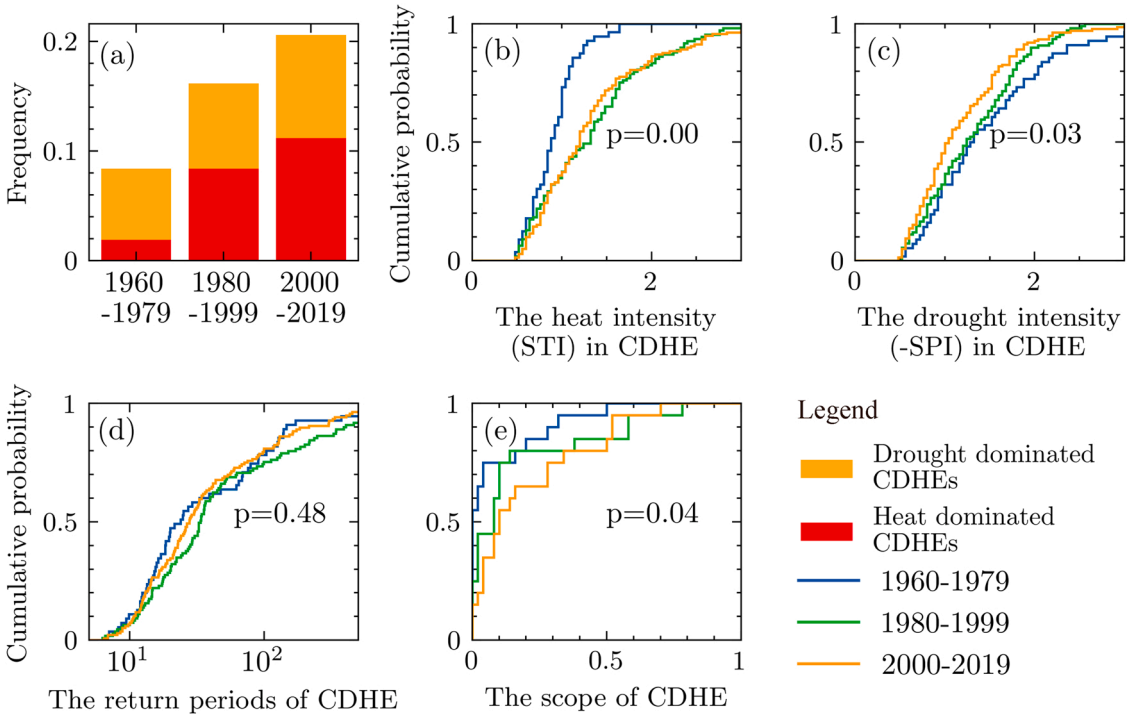

Fig. 7. The characteristics of CDHEs for the periods 1960–1979 (blue), 1980–1999 (green), and 2000–2019 (orange). (a) The occurrence frequency of CDHEs in each time period. Fig. (b)–(e) are the empirical cumulative distribution functions (CDFs) of CDHEs. The x axes represent (b) heat intensity (STI) in CDHEs, (c) drought intensity (-SPI) in CDHEs, (d) the joint return periods of CDHEs, and (e) the scopes of CDHEs.

4. Discussions

4.1. Correlation between precipitation and temperature

Temperature and precipitation showed negative relation in warm season over many regions of world (Zscheischler and Seneviratne, 2017; Gao et al., 2020), which can be driven by the complex land-atmosphere feedbacks and highly related to soil moisture (Chen et al., 2019). For instance, increased temperatures can exacerbate soil moisture deficit, thereby reducing evaporation (Seneviratne et al., 2010). According to energy balance, reduced latent heat flux will lead to increase in sensible heat flux, in turn further raising temperatures (Fischer et al., 2007). Furthermore, increased potential evapotranspiration due to air temperature increases could skew the region towards greater aridity despite precipitation increases (Bennett et al., 2020). In this study, we revealed that the negative correlation between precipitation and temperature was also mainly appeared in warm season in north China. However, in cold season, some stations had significant positive correlation, this may be due to that cold atmosphere with limited water holding capacity reduced precipitation (Berg et al., 2009). We further analyzed the correlation between STI_1 and SPIs when drought (SPI < -0.5) or wetness (SPI > 0.5) happened in July. As shown in Table 3, the correlation coefficients were all negative at 0.01 significant level when drought happened. However, the relationships between STI_1 and SPIs were not significant when wetness (SPI > 0.5) happened. Hence, we can infer that the negative correlation between precipitation and temperature in July is mainly caused by drought (SPI < -0.5) concurrent with heat (STI > 0.5), rather than high SPI concurrent with low STI.

4.2. More frequent and serious CDHEs in north China

The number of CDHEs in summer showed significant increase across many parts of the world, such as the United States (Mazdiyasni and AghaKouchak, 2015), Europe (Sedlmeier et al., 2018), and China (Chen

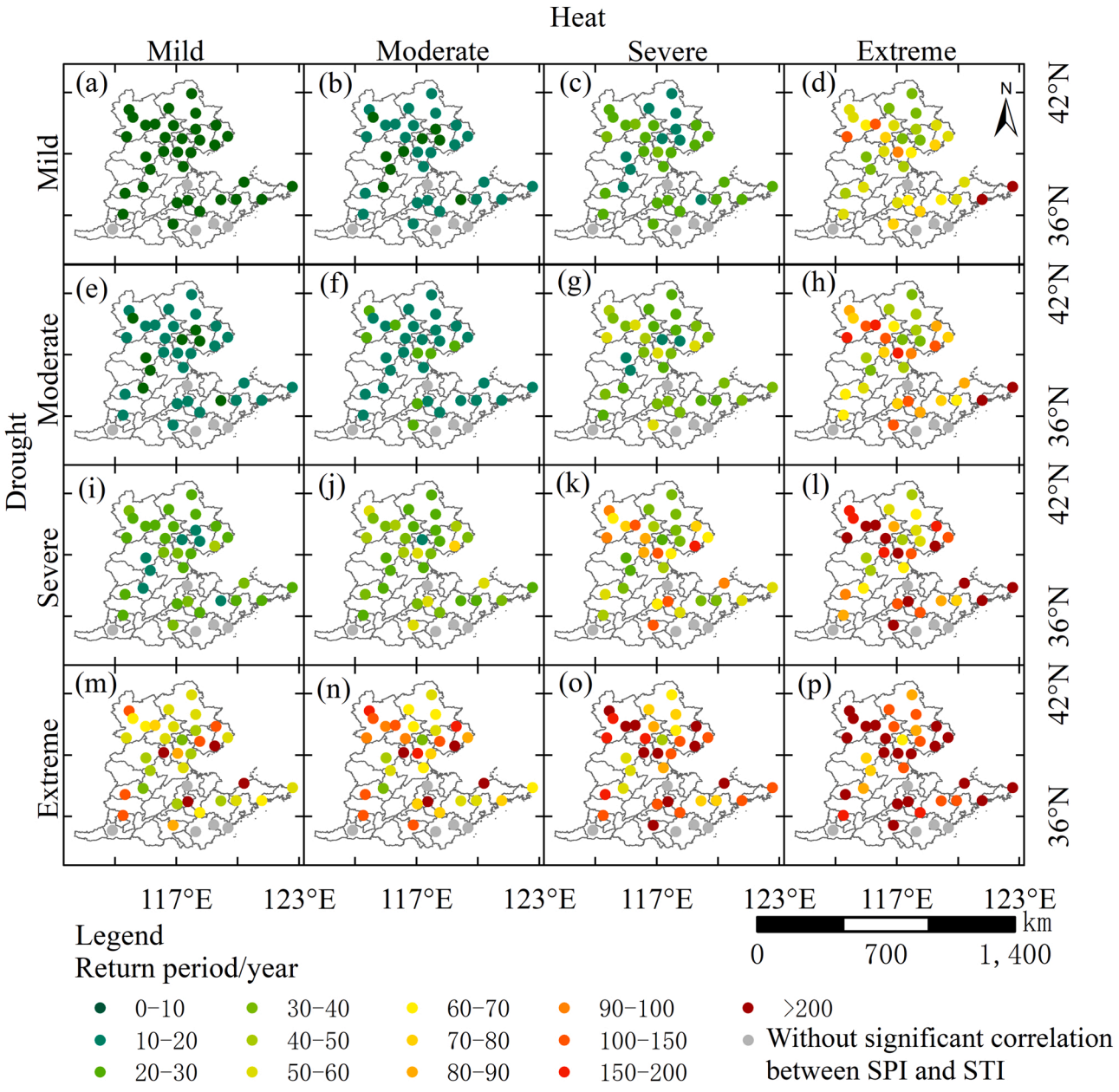

Fig. 8. Spatial distribution of the joint return periods of CDHEs with different drought and heat intensities.

Table 3
Correlation coefficients (r) between STI_1 and SPIs in July.

	r	r (SPI < − 0.5)	r (SPI > 0.5)
SPI_1	-0.25**	-0.17**	-0.05
SPI_2	-0.27**	-0.21**	-0.04
SPI_3	-0.25**	-0.24**	-0.05
SPI_4	-0.25**	-0.19**	-0.06*
SPI_5	-0.25**	-0.19**	-0.06*
SPI_6	-0.25**	-0.19**	-0.06*
SPI_9	-0.25**	-0.17**	-0.03
SPI_12	-0.26**	-0.17**	-0.12**

Note: ** denote the correlation at 0.01 significant level, * denote the correlation at 0.05 significant level. The correlation coefficient between STI_1 and SPIs when SPI < − 0.5 are denoted by r (SPI < − 0.5). The correlation coefficient between STI_1 and SPIs when SPI > 0.5 are denoted by r (SPI > 0.5).

et al., 2019; Wu et al., 2019a). The main trigger for land-atmosphere feedback has shifted from the drought to the extreme temperatures in recent decades (Wu et al., 2019b; Collins, 2021). Our findings further show that more frequent CDHEs with higher intensity and wider spatial extent appeared in 2000–2019 relative to 1960–1979, and this mainly attributed to more serious heats (Fig. 8). Rising global average surface temperatures have been observed over the past few decades (Qiu et al., 2021a), and Wang et al. (2022) shown that the average annual temperature before and after the 1990s was 10.65 °C and 11.49 °C. This leads to an increase in the frequency of extreme heat events (Ababaei and Chenu, 2020; Jakob and Walland, 2016). Although China experienced warming hiatus after 1998, extremes heat still significantly increased (Shen et al., 2018; Li and Amatus, 2020). While there was no significant trend in drought (Wu et al., 2019a). Simulations of future scenarios suggest that the likelihood and extend of CDHEs will increase in future (Wu et al., 2021a, 2021b).

In studying the CDHEs in July, we only studied 3-month scale drought, because this timescale is most closely related to heat in July.

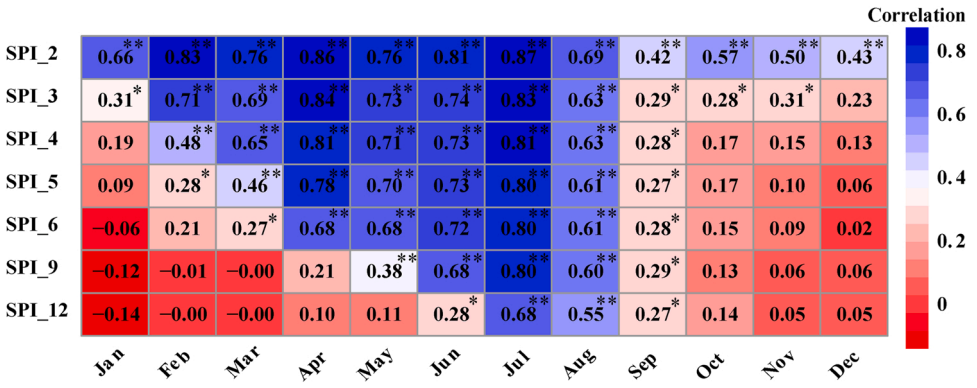

Fig. 9. Correlation coefficients between 1-month scale SPI (SPI_1) and SPI on 2- to 12-month scales (SPI_2 to SPI_12).

Fig. 9 shows the correlation coefficients between SPI_1 and SPIs on other timescales. There were very strong positive correlations between SPI_1 and SPI on 2- to 12-month timescales in July. This means that when July is dry, there is a high probability that the drought has already occurred for a long period. Heat is exacerbated by a prolonged drought, leading to occurrence of CDHEs in July. Hence, although we only studied CDHEs with 3-month scale drought, the results would no significant difference if we used other timescales. We also analyze the characteristics of CDHEs in June (see Figs. S1 and S2 in the Supplementary material), the spatial and temporal characteristics of CDHEs in June shown no big difference with that in July. Our results from July can illustrate the characteristics of CDHEs in north China.

4.3. Relationship between CDHEs and agriculture production in north China

Agriculture is the most sensitive sector to CDHEs. North China is considered as the vital agricultural area, and summer maize growing season last from mid-June to early October in this region (Zhang et al., 2021b). The phenological stage of six leave fully emerged to tasseling for summer maize is most vulnerable to drought and extreme heat, and this stage mainly occurred on July to early August in north China (Zhang et al., 2021b). The present study showed that the CDHEs mainly appeared in June and July in north China. Hence, it tends to be an effective way to mitigate the potential effects of CDHEs by postponing the sowing date of summer maize, so as to make the sensitive tasseling stage occurred at August, when the CDHEs less happened. Xiao et al. (2022) also found that proper delaying sowing date of summer maize can reduce the effects of extreme heat stress on maize production. Our results provide a better understanding of the characteristics of CDHEs, and are essential for developing adaptation strategies to reduce meteorological disaster risk to agricultural productivity.

Agricultural activities may also in turn influence the occurrence of CDHEs in north China. Irrigated agriculture in North China plain has experienced great expansion, which may have significant impact on the surface temperature. Irrigation is one of the main contributors for the risk of high temperature and heatwave in north China (Kang and Eltahir, 2018), and the area equipped for irrigation is much higher in the mid-western region of the North China Plain than other area (Kang and Eltahir, 2018). Heat is the main reason for frequently occurred CDHEs in recent years. So that explains the higher risk of CDHEs in mid-western region (Fig. 8).

5. Conclusions

In summary, we can obtain the following conclusions in this study:

(1) In north China, the proportion of stations with significant negative correlations between SPIs and STI_1 was the most in July, especially for 3-month scale SPI (87 %). The negative correlation was mainly caused by drought (SPI < -0.5) concurrent with heat (STI > 0.5), rather than high SPI concurrent with low STI. Hence July is the month most prone to CDHEs.

(2) Taking 3-month scale drought in July as example, the Symmetrized Joe-Clayton copula was the best to construct the joint dependence probability distribution between drought and heat in most stations. CDHEs were more frequently happened in 2000–2019 with much higher intensity and wider spatial extent, this mainly due to more frequent and severe heats.

(3) The joint return periods of CDHEs in July were relatively shorter in mid-western plain area and north mountainous area over the study period. These two areas were more prone to CDHEs, and the joint return period of CDHEs in both areas were more sensitive to drought intensity.

Our findings provide a better understanding of CDHEs in north China, which is one of the most sensitive and vulnerable regions to global warming and is also a major agricultural production area in China. The findings could offer a valuable reference for disaster risk prevention and future disaster risk preparation.

Declaration of Competing Interest

The authors declare that they have no known competing financial interests or personal relationships that could have appeared to influence the work reported in this paper.

Data Availability

Data will be made available on request.

Acknowledgments

This research was jointly supported by the National Natural Science Foundation of China under Grant no. 41977410, National Key Research and Development Program of China under Grant no. 2019YFC1510205, and the National Natural Science Foundation of China under Grant no. 52179036.

Appendix A. Supporting information

Supplementary data associated with this article can be found in the online version at doi:10.1016/j.agwat.2022.107918.

References

Ababaei, B., Chenu, K., 2020. Heat shocks increasingly impede grain filling but have little effect on grain setting across the Australian wheatbelt. Agric. Meteorol. 284, 107889 https://doi.org/10.1016/j.agrformet.2019.107889.

AghaKouchak, A., Cheng, L., Mazdiyasni, O., Farahmand, A., 2014. Global warming and changes in risk of concurrent climate extremes: Insights from the 2014 California drought. Geophys. Res. Lett. 41, 8847–8852. https://doi.org/10.1002/2014GL062308.

Akaike, H., 2011. Akaike's Information Criterion, fourth ed. Longman, New York.

Allen, C.D., Macalady, A.K., Chenchouni, H., Bachelet, D., McDowell, N., Vennetier, M., Kitzberger, T., Rigling, A., Breshears, D.D., Hogg, E.H., Gonzalez, P., Fensham, R., Zhang, Z., Cobb, N., 2010. A global overview of drought and heat-induced tree mortality reveals emerging climate change risks for forests. For. Ecol. Manag. 259, 660–684. https://doi.org/10.1016/j.foreco.2009.09.

Bandyopadhyay, S., Kanji, S., Wang, L., 2012. The impact of rainfall and temperature variation on diarrheal prevalence in Sub-Saharan Africa. Appl. Geogr. 33, 63–72. https://doi.org/10.1016/j.apgeog.2011.07.017.

Bennett, K.E., Miller, G., Talsma, C., Jonko, A., Bruggeman, A., Atchley, A., Lavadie-Bulnes, A., Kwicklis, E., Middleton, R., 2020. Future water resource shifts in the high desert Southwest of Northern New Mexico. J. Hydrol. Reg. Stud. 28, 100678 https://doi.org/10.1016/j.ejrh.2020.100678.

Berg, P., Haerter, J.O., Thejll, P., Piani, C., Hagemann, S., Christensen, J.H., 2009. Seasonal characteristics of the relationship between daily precipitation intensity and surface temperature. J. Geophys. Res. 114, D18102. https://doi.org/10.1029/2009JD012008.

Chen, L., Chen, X., Cheng, L., Zhou, P., Liu, Z., 2019. Compound hot droughts over China: identification, risk patterns and variations. Atmos. Res. 227, 210–219. https://doi.org/10.1016/j.atmosres.2019.05.009.

Chen, Y., Li, Y., 2017. An inter-comparison of three heat wave types in China during 1961–2010: observed basic features and linear trends. Sci. Rep. 7, 45619. https://doi.org/10.1038/srep45619.

Chretien, J.P., Anyamba, A., Bedno, S.A., Breiman, R.F., Sang, R., Sergon, K., Power,s, A. M., Onyango, C.O., Small, J., Tucker, C.J., Linthicum, K.J., 2007. Drought-associated chikungunya emergence along coastal East Africa. Am. J. Trop. Med. Hyg. 76, 405–407. https://doi.org/10.4269/ajtmh.2007.76.405.

Ciais, P., Reichstein, M., Viovy, N., Granier, A., Ogée, J., Allard, V., Aubinet, M., Buchmann, N., Bernhofer, C., Carrara, A., Chevallier, F., Noblet, N., De, Friend, A.D., Friedlingstein, P., Grünwald, T., Heinesch, B., Keronen, P., Knohl, A., Krinner, G., Loustau, D., Manca, G., Matteucci, G., Miglietta, F., Ourcival, J.M., Papale, D., Pilegaard, K., Rambal, S., Seufert, G., Soussana, J.F., Sanz, M.J., Schulze, E.D., Vesala, T., Valentini, R., 2005. Europe-wide reduction in primary productivity caused by the heat and drought in 2003. Nature 437, 529–533. https://doi.org/10.1038/nature03972.

Collins, B., 2021. Frequency of compound hot–dry weather extremes has significantly increased in Australia since 1889. J. Agron. Crop Sci. 00, 1–15. https://doi.org/10.1111/jac.12545.

Dai, A., 2013. Increasing drought under global warming in observations and models. Nat. Clim. Change 3, 52–58. https://doi.org/10.1038/nclimate1633.

De Boeck, H.J., Dreesen, F.E., Janssens, I.A., Nijs, I., 2011. Whole-system responses of experimental plant communities to climate extremes imposed in different seasons. New Phytol. 189, 806–817. https://doi.org/10.1111/j.1469-8137.2010.03515.x.

Fischer, E.M., Seneviratne, S.I., Vidale, P.L., Lüthi, D., Schär, C., 2007. Soil moisture–atmosphere Interactions during the 2003 European Summer Heat Wave. J. Clim. 20, 5081–5099. https://doi.org/10.1175/JCLI4288.1.

Flannigan, M.D., Krawchuk, M.A., De Groot, W.J., Wotton, B.M., Gowman, L.M., 2009. Implications of changing climate for global wildland fire. Int. J. Wildland Fire 18, 483–507. https://doi.org/10.1071/wf08187.

Gao, X., Gao, M., Yang, Z., Zhu, Q., Xu, Z., Gao, K., 2020. Temperature dependence of extreme precipitation over mainland China. J. Hydrol. 583, 124595 https://doi.org/10.1016/j.jhydrol.2020.124595.

Griffin, D., Anchukaitis, K.J., 2014. How unusual is the 2012–2014 California drought. Geophys. Res. Lett. 41, 9017–9023. https://doi.org/10.1002/2014GL062433.

Hansen, J., Sato, M., Ruedy, R., 2012. Perception of climate change. Proc. Natl. Acad. Sci. USA 109, E2415–E2423. https://doi.org/10.1073/pnas.1205276109.

Hao, Z., Hao, F., Singh, V.P., Xia, Y., Shi, C., Zhang, X., 2018. A multivariate approach for statistical assessments of compound extremes. J. Hydrol. 565, 87–94. https://doi.org/10.1016/j.jhydrol.2018.08.025.

IPCC, 2012. Managing the risks of extreme events and disasters to advance climate change adaptation. A Special Report of Working Groups I and II of the Intergovernmental Panel on Climate Change. Cambridge University Press, Cambridge.

IPCC, 2013. Summary for policymakers of climate change 2013: the physical science basis. Contribution of Working Group I to the Fifth Assessment Report of the Intergovernmental Panel on Climate Change. Cambridge University Press, Cambridge.

Jakob, D., Walland, D., 2016. Variability and long-term change in Australian temperature and precipitation extremes. Weather Clim. Extrem. 14, 36–55. https://doi.org/10.1016/j.wahaoce.2016.11.001.

Kang, S., Eltahir, E.A.B., 2018. North China Plain threatened by deadly heatwaves due to climate change and irrigation. Nat. Commun. 9, 2894. https://doi.org/10.1038/s41467-018-05252-y.

Li, K., Amatus, G., 2020. Spatiotemporal changes of heat waves and extreme temperatures in the main cities of China from 1955 to 2014. Nat. Hazards Earth Syst. Sci. 20, 1889–1901. https://doi.org/10.5194/nhess-20-1889-2020.

Massey, F.J., 1951. The Kolmogorov-Smirnov test for goodness of fit. J. Am. Stat. Assoc. 46, 68–78. https://doi.org/10.1080/01621459.1951.10500769.

Mazdiyasni, O., AghaKouchak, A., 2015. Substantial increase in concurrent droughts and heatwaves in the United States. Proc. Natl. Acad. Sci. USA 112, 11484–11489. https://doi.org/10.1073/pnas.1422945112.

McKee, T.B., Doesken, N.J., Kleist, J., 1993. The relationship of drought frequency and duration to time scale. In: Proceedings of the Preprints, 8th Conference on Applied Climatology. American Meteorological Society, Anaheim, CA, pp. 179–84. ⟨http://ccc.atmos.colostate.edu/relationshipofdroughtfrequency.pdf⟩.

Mellak, S., Souag-Gamane, D., 2020. Spatio-temporal analysis of maximum drought severity using Copulas in Northern Algeria. J. Water Clim. Change 11, 68–84. https://doi.org/10.2166/wcc.2020.070.

Mueller, B., Seneviratne, S.I., 2012. Hot days induced by precipitation deficits at the global scale. Proc. Natl. Acad. Sci. USA, vol. 109, pp. 12398–403. ⟨https://doi.org/10.1073/pnas.1204330109⟩.

Nelsen, R.B., 2007. An Introduction to Copulas, second ed. Springer, New York.

Padmanabha, H., Soto, E., Mosquera, M., Lord, C.C., Lounibos, L.P., 2010. Ecological links between water storage behaviors and Aedes aegypti production: implications for dengue vector control in variable climates. Ecohealth 7, 78–90. https://doi.org/10.1007/s10393-010-0301-6.

Qiu, R.J., Katul, G.G., Wang, J.T., Xu, J.Z., Kang, S.Z., Liu, C.W., Zhang, B.Z., Li, L.A., Cajucom, P.E., 2021a. Differential response of rice evapotranspiration to varying patterns of warming. Agric. For. Meteorol. 298–299, 108293.

Qiu, R.J., Li, L.A., Kang, S.Z., Liu, C.W., Wang, Z.C., Cajucom, P.E., Zhang, B.Z., Agathokleous, E., 2021b. An improved method to estimate actual vapor pressure without relative humidity data. Agric. For. Meteorol. 298–299, 108306.

Qiu, R.J., Li, L.A., Wu, L.F., Agathokleous, E., Liu, C.W., Zhang, B.Z., Luo, Y.F., Sun, S.L., 2022. Modeling daily global solar radiation using only temperature data: past, development, and future. Renew. Sustain. Energy Rev. 163, 112511.

Ribeiro, A.F.S., Russo, A., Gouveia, C.M., Pires, C.A.L., 2020. Drought-related hot summers: a joint probability analysis in the Iberian Peninsula. Weather Clim. Extrem. 30, 100279 https://doi.org/10.1016/j.wace.2020.100279.

Ridder, N.N., Pitman, A.J., Ukkola, A.M., 2020. Do CMIP6 climate models simulate global or regional compound events skillfully. Geophys. Res. Lett. 48, e2020GL091152 https://doi.org/10.1029/2020GL091152.

Sedlmeier, K., Feldmann, H., Schädler, G., 2018. Compound summer temperature and precipitation extremes over central Europe. Theor. Appl. Climatol. 131, 1493–1501. https://doi.org/10.1007/s00704-017-2061-5.

Seneviratne, S.I., Corti, T., Davin, E.L., Hirschi, M., Jaeger, E.B., Lehner, I., Orlowsky, B., Teuling, A.J., 2010. Investigating soil moisture-climate interactions in a changing climate: a review. Earth Sci. Rev. 99, 125–161. https://doi.org/10.1016/j.earscirev.2010.02.004.

Shen, X., Liu, B., Lu, X., 2018. Weak cooling of cold extremes versus continued warming of hot extremes in China during the recent global surface warming hiatus. J. Geophys. 123, 4073–4087. https://doi.org/10.1002/2017JD027819.

Shukla, S., Safeeq, M., AghaKouchak, A., Guan, K., Funk, C., 2015. Temperature impacts on the water year 2014 drought in California. Geophys. Res. Lett. 42, 4384–4393. https://doi.org/10.1002/2015GL063666.

Wang, F., Lai, H., Li, Y., Feng, K., Zhang, Z., Tian, Q., Zhu, X., Yang, H., 2022. Dynamic variation of meteorological drought and its relationships with agricultural drought across China. Agric. Water Manag. 261, 107301 https://doi.org/10.1016/j.agwat.2021.107301.

Wazneh, H., Arain, M.A., Coulibaly, P., Gachon, P., 2020. Evaluating the dependence between temperature and precipitation to better estimate the risks of concurrent extreme weather events. Adv. Meteor. 12, 8763631. https://doi.org/10.1155/2020/8763631.

Williams, A.P., Allen, C.D., Millar, C.I., Swetnam, T.W., Michaelsen, J., Still, C.J., Leavitt, S.W., 2010. Forest responses to increasing aridity and warmth in the southwestern United States. Proc. Natl. Acad. Sci. USA 107, 21289–21294. https://doi.org/10.1073/pnas.0914211107.

Wolf, S., Keenan, T.F., Fisher, J.B., Baldocchi, D.D., Desai, A.R., Richardson, A.D., Scottg, R.L., Lawh, B.E., Litvaki, M.E., Brunsellj, N.A., Petersk, W., van der Laan-Luijkx, I.T., 2016. Warm spring reduced carbon cycle impact of the 2012 US summer drought. Proc. Natl. Acad. Sci. USA 113, 5880–5885. https://doi.org/10.1073/pnas.1519620113.

Wu, X., Hao, Z., Hao, F., Li, C., Zhang, X., 2019a. Spatial and temporal variations of compound droughts and hot extremes in China. Atmosphere 10, 95. https://doi.org/10.3390/atmos10020095.

Wu, X., Hao, Z., Hao, F., Zhang, X., 2019b. Variations of compound precipitation and temperature extremes in China during 1961–2014. Sci. Total. Environ. 663, 731–737. https://doi.org/10.1016/j.scitotenv.2019.01.366.

Wu, X., Hao, Z., Zhang, Y., Zhang, X., Hao, F., 2021a. Anthropogenic influence on compound dry and hot events in China based on coupled model intercomparison project phase 6 models. Int. J. Clim. 1–12. https://doi.org/10.1002/joc.7473.

Wu, Y., Miao, C., Sun, Y., AghaKouchak, A., Shen, C., Fan, X., 2021b. Global observations and CMIP6 simulations of compound extremes of monthly temperature and precipitation. GeoHealth 5, e2021GH000390. https://doi.org/10.1029/2021GH000390.

Xiao, D., Bai, H., Liu, D.L., et al., 2022. Projecting future changes in extreme climate for maize production in the North China Plain and the role of adjusting the sowing date. Mitig. Adapt. Strateg. Glob. Change 27, 21.

Xu, Y., Zhang, X., Hao, Z., Hao, F., Li, C., 2021. Projections of future meteorological droughts in China under CMIP6 from a three-dimensional perspective. Agr. Water Manag. 252, 106849 https://doi.org/10.1016/j.agwat.2021.106849.

Yao, N., Li, Y., Lei, T., Peng, L., 2018. Drought evolution, severity and trends in mainland China over 1961–2013. Sci. Total Environ. 616, 73–89. https://doi.org/10.1016/j.scitotenv.2017.10.327.

Zhang, H., Wu, C., Yeh, P.F., Hu, B.X., 2020. Global pattern of short-term concurrent hot and dry extremes and its relationship to large-scale climate indices. Int. J. Climatol. 40, 5906–5924. https://doi.org/10.1002/joc.6555.

Zhang, Q., Han, J., Yang, Z., 2021a. Hazard assessment of extreme heat during summer maize growing season in Haihe Plain, China. Int. J. Clim. 41, 4794–4803. https://doi.org/10.1002/joc.7099.

Zhang, Q., Han, J., Yang, X.Y., 2021b. Effects of direct heat stress on summer maize and risk assessment. Theor. Appl. Climatol. 146, 755–765.

Zhu, Y., Liu, Y., Wang, W., Singh, V.P., Ma, X., Yu, Z., 2019. Three dimensional characterization of meteorological and hydrological droughts and their probabilistic links. J. Hydrol. 578, 124016 https://doi.org/10.1016/j.jhydrol.2019.124016.

Zscheischler, J., Seneviratne, S.I., 2017. Dependence of drivers affects risks associated with compound events. Sci. Adv. 3, e1700263 https://doi.org/10.1126/sciadv.1700263.

Zscheischler, J., Michalak, A.M., Schwalm, C., Mahecha, M.D., Huntzinger, D.N., Reichstein, M., Berthier, G., Ciais, P., Cook, R.B., El-Masri, B., Huang, M., Ito, A., Jain, A., King, A., Lei, H., Lu, C., Mao, J., Peng, S., Poulter, B., Ricciuto, D., Shi, X., Tao, B., Tian, H., Viovy, N., Wang, W., Wei, Y., Yang, J., Zeng, N., 2014. Impact of large-scale climate extremes on biospheric carbon fluxes: an intercomparison based on MsTMIP data. Glob. Biogeochem. Cycles 28, 585–600. https://doi.org/10.1002/2014GB004826.

Zscheischler, J., Martius, O., Westra, S., Bevacqua, E., Raymon, C., Horton, R.M., Van den Hurk, B., AghaKouchak, A., Aglaé, J., Mahecha, M.D., Maraun, D., Ramos, A.M., Ridder, N.N., Thiery, W., Vignotto, E., 2020. A typology of compound weather and climate events. Nat. Rev. Earth Environ. 1, 333–347. https://doi.org/10.1038/s43017-020-0060-z.